Turkish Archives of Pediatrics

REVIEW
DOI: 10.5152/TurkArchPediatr.2022.22085

Imaging of Central Nervous System Involvement in Pediatric Hematologic Disorders

Sevinç Kalın[1], Korgün Koral[2]

[1]Department of Pediatric Radiology, University of Health Sciences Umraniye Training and Research Hospital, İstanbul, Turkey
[2]Division of Pediatric Radiology, University of Texas Southwestern Medical Center, Texas, USA

ABSTRACT

Hematologic disorders and malignancies are commonly encountered in children. The central nervous system is affected by many benign and malignant hematological diseases. Neurologic findings may occur due to central involvement of hematological disease or neurotoxic effects of treatment during the disease. At all these stages, radiological imaging and evaluation have a critical role. In this review article, we aim to describe the imaging findings of central nervous system involvement in pediatric hematologic diseases. This review was prepared based on the latest literature available in the PubMed database in the English language from inception to March 2022. The radiological images of the patients in our archive were obtained from the PACS (Picture Archiving and Communication Systems) to set an example for the diseases described in the text.

Keywords: Central nervous system, hematologic disorders, imaging, neurotoxicity

INTRODUCTION

Hematologic disorders and malignancies are commonly encountered in children. Central nervous system (CNS) involvement is observed in many hematological diseases, especially in the malignant group. Neuroimaging plays an important role in the diagnosis of nervous system findings due to hematologic involvement or the neurotoxic effects of treatment. For a good radiological evaluation, sufficient information should be obtained about the patient's clinic and treatments. In this review article, we aim to describe the imaging findings of CNS involvement in pediatric hematologic diseases.

CNS INVOLVEMENT IN HEMATOLOGIC DISORDERS

Hemorrhagic and Coagulation Disorders

Hemorrhagic disorders may result from disturbances of one or more of the factors involved in hemostasis. It can be classified under the main headings as follows: vasculopathies (hereditary, secondary, and allergic), platelet disorders (thrombocytopenia, thrombocytosis, functional abnormalities), coagulation disorders caused by coagulation factor deficiencies (hemophilia A and hemophilia B), and hyperfibrinolysis.[1]

Osler–Weber–Rendu disease, also known as hereditary hemorrhagic telangiectasia, from the vasculopathy group, is an autosomal dominant disease characterized by multiple arteriovenous malformations (AVMs). AVM is composed of thin and convoluted vessels that rupture and bleed easily.[2] Arteriovenous malformation appears as isodense serpentine vessels on noncontrast brain computed tomography (CT). T1-weighted (T1W) and T2-weighted (T2W) magnetic resonance imaging (MRI) shows vessels with flow gaps and possible hemorrhages. Edema, mass effect, and peripheral gliosis may be demonstrated on FLAIR A and T2W sequences.[3]

Corresponding author:
Sevinç Kalın
✉svnctsr@yahoo.com
Received: April 11, 2022
Accepted: March 29, 2022

Cite this article as: Kalın S, Koral K. Imaging of central nervous system involvement in pediatric hematologic disorders. *Turk Arch Pediatr.* 2022;57(3):267-281.

The Ehlers–Danlos syndrome is another hereditary vasculopathy. Vessel wall fragility and microvascular hemorrhages may be seen secondary to collagen deformation (intraparenchymal and subarachnoid hemorrhages). Most important and common cerebrovascular complications are carotid-cavernous fistulas and arterial dissections.[4,5]

Many predisposing factors such as infections, drugs, metabolism disorders and connective tissue diseases affect the vessel wall and cause bleeding. Proximal middle cerebral artery (MCA) and posterior perforated arteries are the most commonly affected vessels. We can use contrast-enhanced T1W images for meningeal inflammatory changes, diffusion-weighted images (DWIs) for cerebritis and infarcts, and sensitivity-weighted images (SWIs) for microhemorrhages. Also in septicemia, bleeding secondary to disseminated intravascular coagulation may occur.[1]

Thrombocytopenic purpura is a disease of unknown etiology caused by antiplatelet antibodies. The acute condition usually occurs in young children and after an acute febrile illness. The most common CNS findings are subarachnoid and intracranial bleeding is observed.[6]

Coagulation factor deficiency or dysfunction excluding factor XII may cause hemorrhagic disorders. Hemophilia A and hemophilia B diseases are seen in the deficiency of factor VII and factor IX in the common pathway, respectively. Acute bleeding is hyperdense on CT (Figure 1). Today, primarily SWI and DWI sequences are preferred. In the chronic process, cerebral atrophy, calcifications, and multifocal hyperintensities are observed in the cerebral white matter on T2W images.[1]

Protein C and S Deficiency

Protein C is a vitamin K-dependent anticoagulant. Protein S is a cofactor for activated protein C.[7] The activated protein C/protein S complex proteolyzes procoagulant factors V and VIII. Thus, factor X and prothrombin activation are prevented and fibrin formation is delayed.[8] Deficiency of these factors is inherited autosomal dominant and is associated with an increased risk of venous thrombosis[9,10] (Figure 2). Homozygous cases are usually present in neonates with purpura fulminans. Heterozygous cases can range from varying degrees of venous thromboembolism to embolic complications. There are no specific radiographic features while imaging thrombotic and embolic complications.[9]

Sickle Cell Disease

Sickle cell disease (SCD) is inherited autosomal recessively and results in abnormal hemoglobin S (Hgb S) production as a result of defects in the formation of normal hemoglobin A. In the deoxygenated state, Hgb S forms aggregates causing red blood cells (RBCs) to lose their normal discoid biconcave shape, a process called sickling. The abnormal RBCs increase the tendency for thrombosis and result in vascular occlusions and finally organ damage.[11] Magnetic resonance imaging is a useful and first-choice imaging modality for both silent and clinical infarctions. In these patients, infarctions are frequently observed in the white matter and peripheral feeding regions of the anterior cerebral arteries and MCAs.[12]

In SCD, the most common neurological complication is stroke which develops due to vasculopathy and thrombosis. Infarction is usually ischemic. Embolic and thrombotic strokes are unusual. Diffusion-weighted imaging is performed in the acute period and pathological findings are shown even in the first 6 hours. Between 1 week and 1 month, infarcts are only slightly hypointense on T1W images and hyperintense on T2W images. In the chronic phase, signs of focal atrophy develop (Figure 3a). At CT, infarcts show areas of low attenuation in the acute phase and atrophic findings are observed over time.[13]

It is possible to evaluate large cerebral artery flow dynamics with transcranial Doppler ultrasonography (US) to identify patients at risk of stroke to initiate preventive therapy. Studies show that high velocities (velocities above 170–200 cm/s) in the distal internal carotid artery and proximal MCA are associated with an increased risk of stroke. Transcranial Doppler US scanning begins at age 3 and maintenance of transfusion therapy is given to high-rate patients on two consecutive examinations.[14]

Stroke is responsible for approximately 12% of deaths in patients with SCD.[15] Computed tomography angiography (CTA) may be used; however, its utilization in children is controversial due to ionizing radiation. Magnetic resonance arteriography (MRA) is the imaging modality of choice in the evaluation of

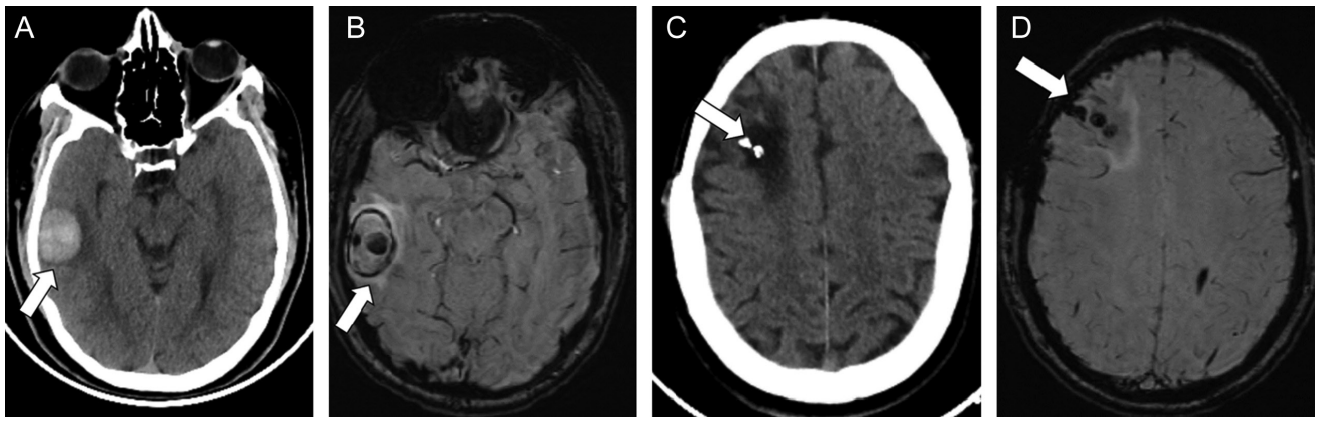

Figure 1. A 13-year-old male diagnosed with Factor XIII deficiency has an acute hematoma in the right temporal lobe is seen on axial CT (a) and SWI (b) images. In the same patient, there is an encephalomalastic area secondary to the previous hemorrhage accompanied by calcifications in the right frontal lobe (c, d).

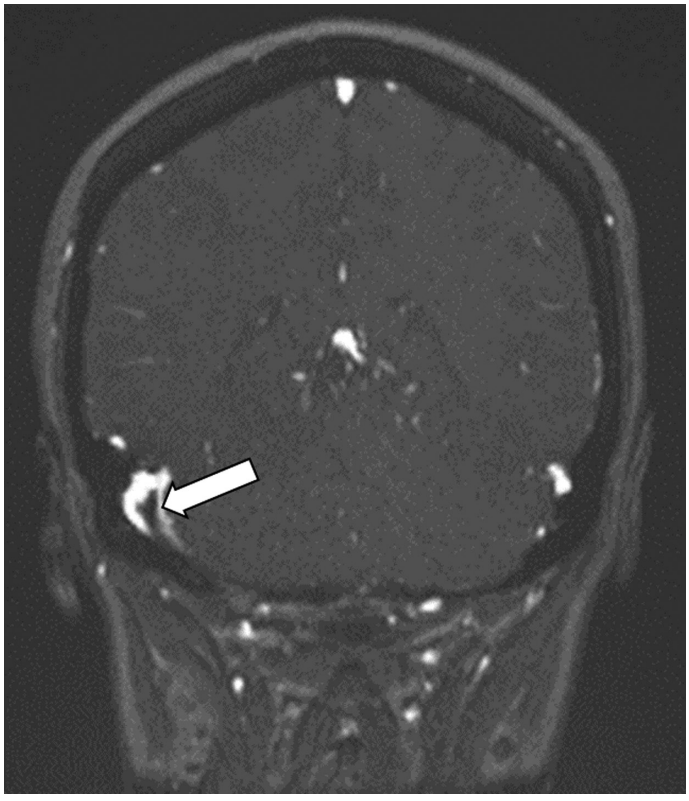

Figure 2. A 17-year-old male with protein C deficiency. 2D time of flight magnetic resonance venography image shows nonocclusive thrombus within the dominant right sigmoid sinus.

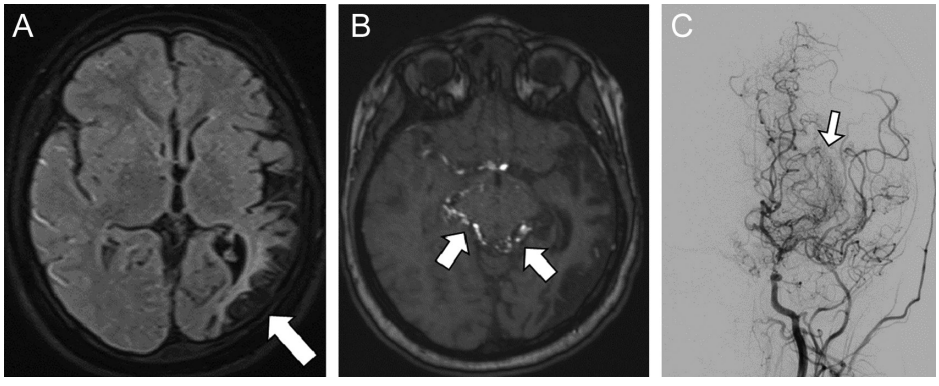

Figure 3. In the axial FLAIR-W images of the patient with Moyamoya syndrome, a continuous chronic ischemic encephalomalasic area is observed in the left temporooccipital region (a). Perimesencephalic collateral vascular structures are selected in axial post-contrast T1W images (b). In the diagnostic angiography examination of the patient, collateral vascular structures that create a puff of smoke appearance are observed (c).

SCD vasculopathy. While small caliber arterial disease is difficult to diagnose with MRA, the larger vessels can be adequately assessed without administering contrast material.

Due to chronic and progressive stenosis and occlusion of the internal carotid arteries and their proximal branches, multiple collaterals may develop at the base of the brain resulting in Moyamoya syndrome.[16] Collateral multiple small abnormal net-like vessels give a characteristic "puff of smoke" appearance on angiography. Due to the lower flow and spatial resolution in CTA and MRA, this view is not always shown[17] (Figure 3). Moyamoya syndrome refers to the typical Moyamoya vasculopathy plus associated conditions such as SCD or neurofibromatosis type I.[16] In a large group of patients (n, 5516), Thangarajh et al defined vasculopathy on MR angiography in 10.3% of asymptomatic children with SCD.[18] Diffusion-weighted imaging allows for evaluation of acute ischemic injuries in children with SCD[19] (Figure 4).

Thalassemia

It is an autosomal recessive hemoglobinopathy that causes microcytic anemia occurring in the Mediterranean region. Severe anemia secondary to ineffective hematopoiesis causes bone marrow enlargement and conversion of yellow marrow

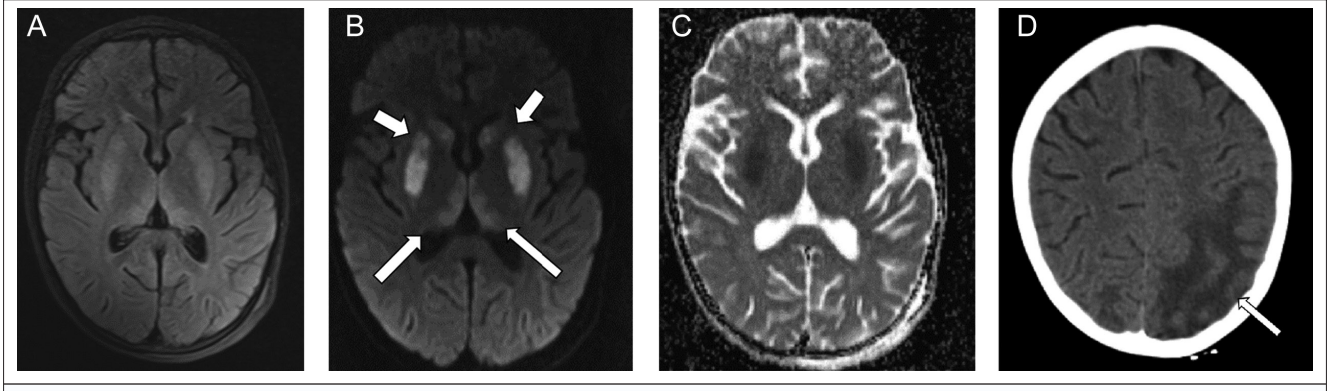

Figure 4. Signal changes consistent with ischemia are observed in the bilateral basal ganglia and ventromedial of the thalamus in FLAIR W (a) diffusion-weighted images (b) and ADC mapping (c) in a patient diagnosed with sickle cell anemia who applied to the emergency department with acute neurological findings. An area of acute ischemic tissue is observed in the posterior parietal at the vertex level in the non-contrast CT examination performed in the emergency department at a different time (d).

to red marrow As in sickle cell anemia, the medullary spaces of bones expand and the cortical bone thins[20,21] (Figure 5).

Osteopenia and osteoporosis develop by causing cortical and trabecular thinning and destruction of medullary trabeculae. In the cranium, the occipital bone is spared due to lack of hemopoietic bone marrow. Classic appearance of the cranium 'hair-on-end' is rare in children over 9 years of age and under treatment.[20]

Extramedullary hematopoiesis develops as a response to failure of erythropoiesis in the bone marrow. It usually affects internal organs such as the liver, spleen, and lymph nodes and includes the thorax. Less commonly, it can affect the pleura, lungs, gastrointestinal tract, breast, skin, brain, kidneys, and adrenal glands. Anemia, splenectomy, and thrombocytosis are the risk factors in the development of infarction in silent cerebral ischemia in thalassemia patients.[22] Occasional blood transfusion/regular transfusion has been cited as an important preventative.[23]

Regular blood transfusion is needed from the first year of life in thalassemia major. Chelation therapy is performed, and iron accumulation occurs in various tissues. Although there is often cardiac and endocrinological involvement, another tissue at risk is the nervous system.[24-26]

Among the CNS lesions, iron accumulation in the basal ganglia, millimetric ischemic foci due to hypoxia, thromboembolism, dura mater thickening due to extramedullary hematopoiesis, and cerebral atrophy can be observed. The most common finding on cranial MRI is basal ganglia calcifications. Iron deposition has also been demonstrated in the thalamus, red nucleus, and choroid plexus. The second most common cranial

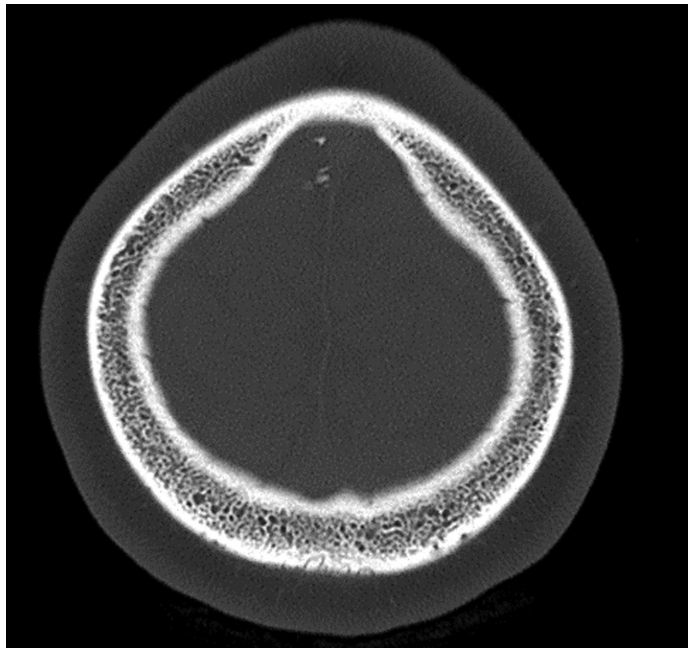

Figure 5. Axial head computed tomography in bone window shows characteristic expansion of the calvarial bone marrow in sickle cell disease.

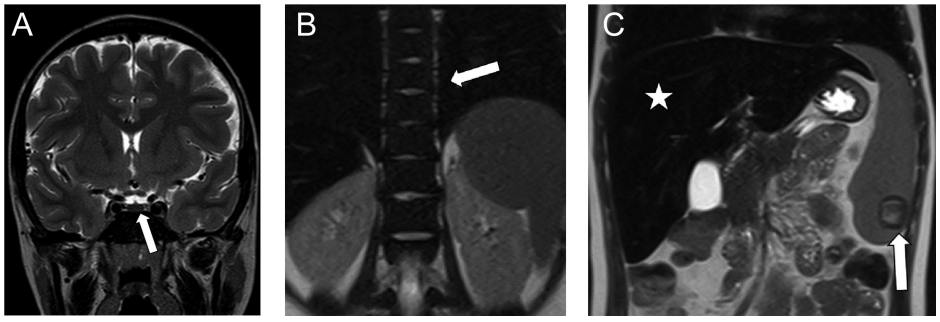

Figure 6. 15-year-old with thalassemia. Coronal T2-weighted (T2W) image show marked T2 hypointensity within the pituitary gland due to iron accumulation secondary to chronic blood transfusions. There is marked expansion and T2 hypointensity of the calvarial and skull base bone marrow. A 14-year-old girl with a diagnosis of thalassemia, hypointensity is observed in the vetebral bone marrow (b) and liver (c) in T2W images secondary to coronal iron deposition. The same patient has a nodular lesion consistent with extramedullary hematopoiesis in the spleen (c).

MRI pathology is millimetric ischemic changes.[25] While extramedullary hematopoiesis is more common in other parts of the body, it is rare intracranially (Figure 6).

CNS Involvement in Langerhans Cell Histiocytosis

Langerhans cell histiocytosis (LCH) is a rare multisystem disease with a wide clinical spectrum. The true incidence is unknown, as many patients remain undiagnosed. The disease is more common in the pediatric population, with a peak incidence between 1 and 3 years of age with a male predilection (M : F ~ 1.5 : 1).[27]

CNS involvement of LCH is uncommon and poorly understood. The most common sites of CNS involvement with LCH are the pituitary infundibulum and hypothalamus, resulting in diabetes insipidus at presentation. A lack of T1W high signal intensity of the posterior pituitary and enhancement of thickened infundibulum are characteristic but nonspecific findings[28] (Figure 7). Especially sagittal pre- and post-contrast T1W sequences are important in diagnosis. The primary differential consideration of LCH when it involves the hypothalamic–pituitary axis is germinoma. In the absence of additional foci of involvement for both entities, discriminating one from the other is nearly impossible on imaging. Magnetic resonance imaging with contrast is the modality of choice for diagnosis and follow-up of intracranial LCH.[29]

Neurodegenerative LCH refers to poorly understood condition that may be encountered at any time following the intitial diagnosis of LCH. Cerebellum, brain stem, optic chiasm, basal ganglia, and cerebral hemispheres may be involved. While some lesions may show enhancement, typically there is volume loss, confluent gliosis of the white matter, and calcifications of deep gray matter structures, particularly the cerebellar dentate nuclei.[30]

Hemaphagocytic Lymphohistiocytosis

Hemaphagocytic lymphohistiocytosis (HLH) is a heterogeneous disorder characterized by toxic uncontrolled immune activation.[31] This immune activation is often driven by genetic mutations occurring along the perforin-dependent granule exocytosis pathway and is referred to as primary HLH.[32] In secondary HLH, there is no underlying genetic mutation but systemic inflammation or immunotherapy may cause macrophage activation.

In children with HLH, MR imaging findings frequently overlap with those of infection, inflammation, or demyelination, causing delay in diagnosis and treatment. A myriad of nonspecific imaging findings have described in HLH, including regions of confluent or focal T1 and T2 prolongation which may demonstrate enhancement (Figure 8). There may be involvement of the cerebral hemispheres, deep gray matter structures, brain

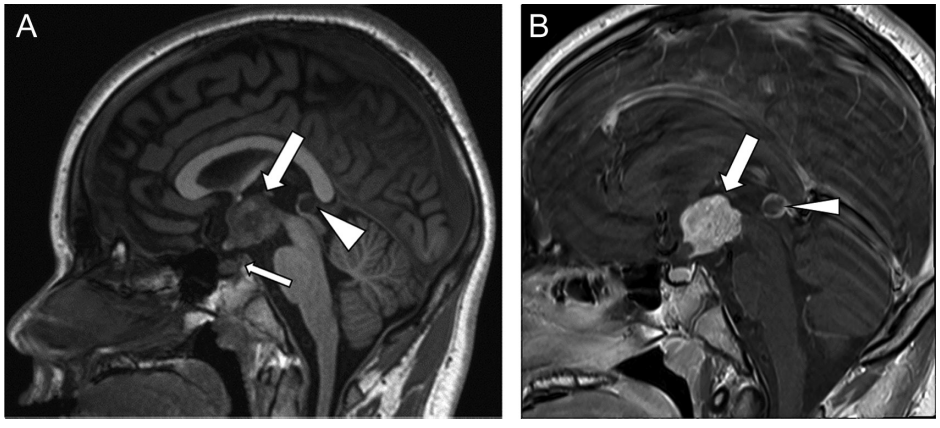

Figure 7. An 11 year-old female diagnosed with LCH, presented with diabetes insipidus. There is lack of visualization of the normal neurohypophysis (a, thin arrow) in pre-contrast sagittal T1W images. The suprasellar mass demonstrates heterogenous, intense enhancement (thick arrow). Incidental note is made of a pineal cyst (arrow head).

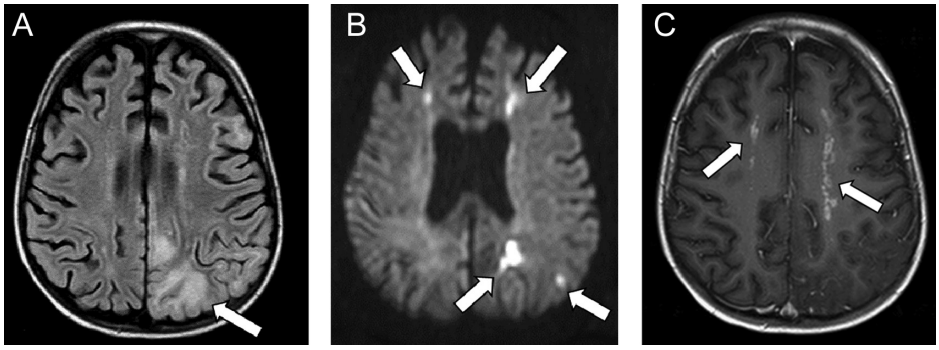

Figure 8. A 2-year-old male diagnosed with hemaphagocytic lymphohistiocytosis, hyperintense areas forming confluence are observed in the subcortical and peiventricular white matter in the left posterior parietal in axial FLAIR-W images (a). In diffusion-weighted studies, there are signal changes consistent with periventricular and subcortical millimetric ischemic diffusion limitations (b). In post-contrast axial T1-weighted images, contrast enhancements in the periventricular white matter at the centrum semiovale level are remarkable (c).

stem, and cerebellum. Occasionally, mass-like lesions are encountered. Cranial nerve involvement has been reported.[31]

CNS INVOLVEMENT IN HEMATOLOGIC MALIGNANCIES

Leukemia

Leukemia is the most common malignancy of childhood and constitutes 25–30% of all pediatric malignancies. Acute lymphoblastic leukemia (ALL) is the most common type accounting for 85% of all pediatric leukemias.[33] CNS is one of the so-called sanctuary sites for leukemia along with testicles and kidneys.[34]

CNS involvement is less than 5% of B-ALL and 10–15% of T-ALL cases at the time of diagnosis. The detection of CNS involvement in ALL is essential for CNS-targeted therapy.[35]

Cerebrospinal fluid (CSF) cytology is the primary diagnostic test for CNS involvement in pediatric leukemia. MRI is not routinely indicated for assessment of CNS involvement. While CT without contrast may be used in evaluation of acute events (such as intracranial hemorrhage, dural venous sinus thrombosis, and ischemic stroke), MRI is more frequently used for the evaluation of the complications encountered during therapy. Mass-like involvement in leukemia referred to as chloroma is rare in children.[36] Chloroma can involve the extraaxial spaces (epidural or subdural), meninges, or parenchyma of the brain or spinal cord (Figure 9). More commonly, complications related to the primary disease (hemorrhage or stroke) or related to therapy are seen (methotrexate toxicity or L-asparaginase toxicity).[37] It is not uncommon to encounter cerebral and cerebellar volume loss, white matter injury, and microhemorrhages in asymptomatic pediatric leukemia survivors.[38]

Methotrexate toxicity is usually encountered 3-14 days after intrathecal administration.[39] Although less common, methotrexate toxicity can be seen following intravenous administration as well. The patients were present with acute neurological deterioration. Diffusion-weighted images are particularly useful in the diagnosis of acute methotrexate toxicity, excluding stroke in patients with leukemia. While ischemic stroke involves a vascular territory, the lesions related to the methotrexate toxicity are generally bilateral, periventricular (involving the centrum semiovale and corona radiata), and do not conform to a single vascular territory. In general, the transient hyperintense signal is observed on T2W and FLAIR-weighted MRI sequences in the white matter at the level of the bilateral centrum semiovale. Subcortical U fibers are preserved. Characteristically, reversible signal changes consistent with cytotoxic edema are observed on DWI MRI in the defined areas. These DWI changes are considered reliable and early manifestations of acute methotrexate-related leukoencephalopathy (Figure 10). Dural venous sinus thrombosis is encountered less commonly than acute methrotrexate toxicity, but it is most frequently associated with L-asparaginase therapy.[40] L-Asparaginase leads to the depletion of plasma proteins involved in both coagulation and fibrinolysis, causing cortical infarction, dural sinus thrombosis, intracerebral hemorrhage, or infarctions[41] (Figure 11).

The risk of opportunistic infections increases in neutropenic periods. Imaging appearance of infections seen in leukemic patients is not different than those seen in the general population. The sinonasal regions should be investigated closely as these could be the sites for direct extension of infection to the CNS.[42]

It is possible to evaluate bone marrow infiltrates in craniofacial bones and vertebra with brain MRI and spinal MRI (Figure 9e). With contrast-enhanced brain MRI and DWI, bone marrow signal, cortical expansion, erosions, and soft tissue masses can be demonstrated.[43] Mineralizing microangiopathy, one of the effects of radiation therapy, is an imaging complication that is occasionally encountered in pediatric leukemia survivors.[43] As a side effect of radiotherapy, hyalinization and fibrinoid necrosis of small arteries and arterioles develop secondary to endothelial proliferation and calcium deposition.[34,44] The patients are generally asymptomatic, and symmetrical calcifications are seen on CT involving the basal ganglia and subcortical white matter in children previously treated with radiation therapy and intrathecal methotrexate (Figure 12).

Lymphoma

Central nervous system lymphoma occurs as an isolated primary lesion or as a secondary involvement of systemic lymphoma.

Primary CNS Lymphoma

Primary CNS lymphoma (PCNSL) is a form of extranodal, high-grade, non-Hodgkin B-cell neoplasm and rarely spreads

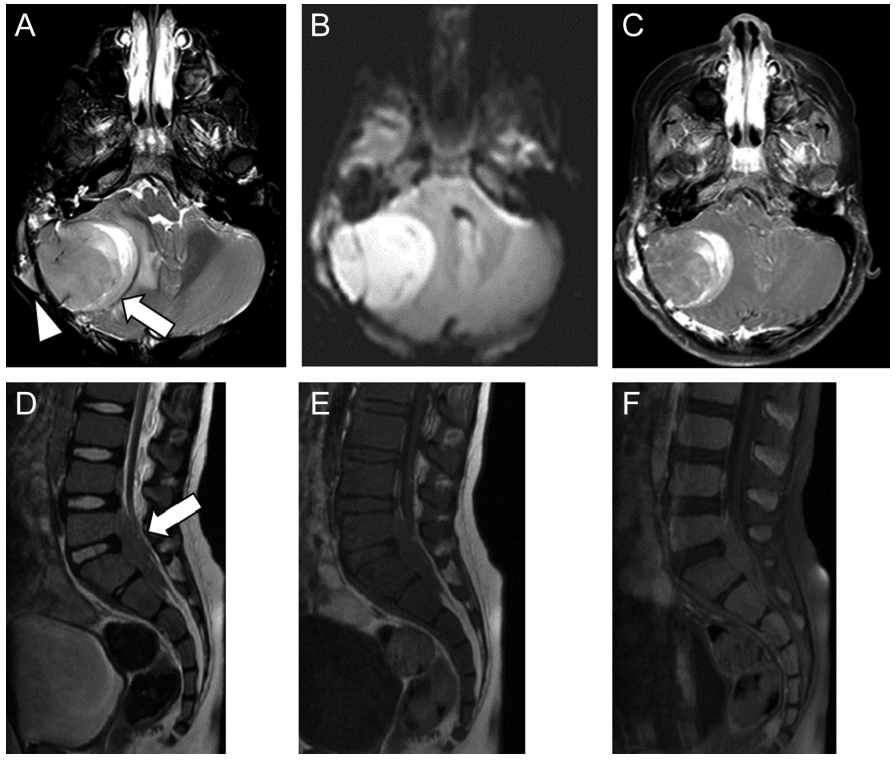

Figure 9. A 4-year-old male diagnosed with ALL, in the axial plane T2W, diffusion, and post-contrast T1W images, respectively, there is an extraaxially posterior fossa solid mass (arrow) with subperiosteal component (arrowhead). There is a cytotoxic edema effect by pressing the right cerebellar hemispheres and brain stem with diffusion restriction (b) and heterogeneously contrasting (c). A 4-year-old patient with a diagnosis of ALL has a solid mass lesion in the spinal canal extradurally at L5-S2 levels in sagittal T2W (d), pre (e) and post-contrast T1W images (f), developed during the follow-up. Hypointencity of vertebrae is also seen on T1W images secondary to diffuse leukemic bone marrow infiltration.

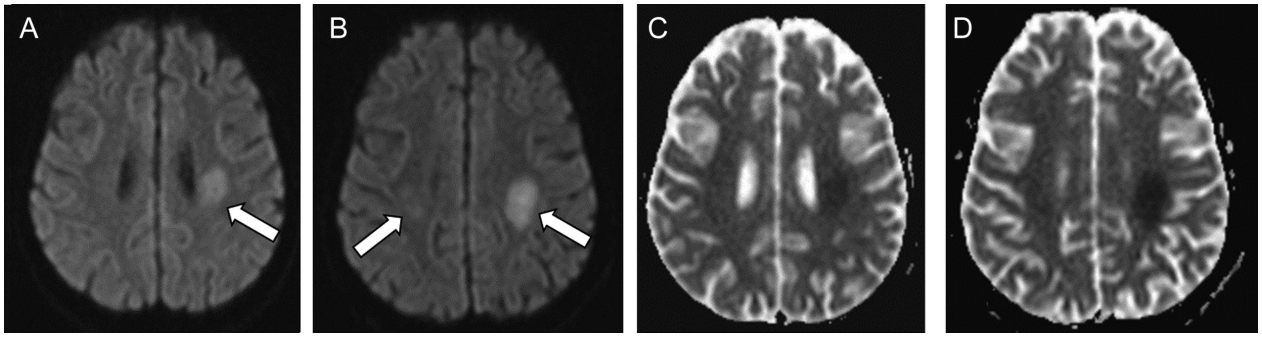

Figure 10. Bilateral periventricular nodular diffusion restriction is observed at centrum semiovale and corona radiata levels in diffusion-weighted images (a,b) and ADC maps (d,e) in a 12-year-old male who received intrathecal treatment 5 days ago.

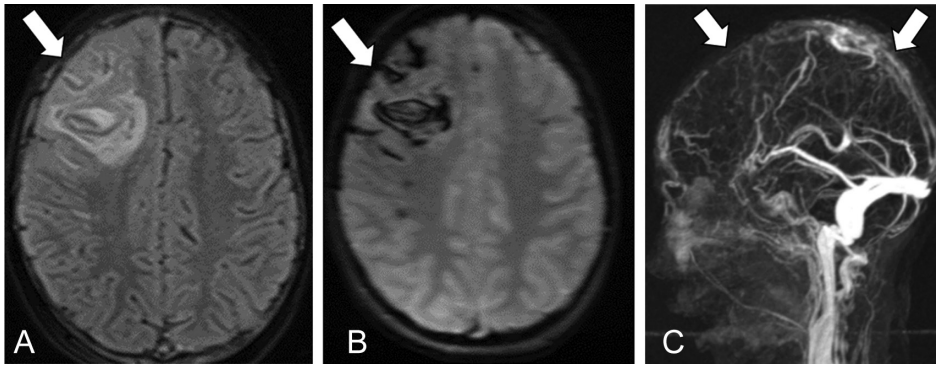

Figure 11. In a 7-year-old male with ALL, a cortical-subcortical hemorrhagic infarct in the right frontal lobe secondary to superior sagittal sinus thrombosis is observed in the images of T2W (a), SWI (b), and MR venography (c).

Figure 12. In a 4-month-old male with ALL, unenhanced axial CT scan shows multiple dystrophic calcifications at bilateral periventricular white matter secondary to mineralized microangiopathy.

outside the nervous system, typically involving the brain parenchyma with less frequent involvement of the leptomeninges, spinal cord, pituitary gland, cranial nerves, and the orbita. It is a rare tumor that accounts for 2-6% of all primary brain tumors and 1-2% of all non-Hodgkin lymphomas. Unlike adults, PCNSL is extremely rare in children.[45,46] The most common presentation is a single intracranial mass, most commonly located supratentorially in the white matter of the frontal and parietal lobes. Basal ganglia are involved in 13-20% of patients[45] (Figure 13).

Immunocompromised patients are at increased risk for developing primary CNS lymphoma. In this group, it may be difficult to distinguish PCNSL from the more common cerebral toxoplasmosis. Both of them can present with multiple ring-enhancing lesions on CT and MRI. Perfusion MRI and MRI spectroscopy can be used to differentiate CNS lymphomas from other brain lesions.[47]

PCNSL lesions cause diffusion restriction secondary to high cellularity and appear hyperintense on DWI and hypointense on apparent diffusion coefficient (ADC) maps (Figure 9). However, this imaging feature may not necessarily help in discriminating PCNSL from toxoplasmosis as there is a significant overlap in the ADC values of these two entities.[48]

Secondary CNS Lymphoma

While secondary CNS lymphoma is not uncommon in adults, it is rare in children.[49] CNS involvement by systemic lymphoma presents as leptomeningeal disease in 60-70% of patients (Figure 14). Less common parenchymal CNS involvement in systemic lymphoma can present as single or multiple parenchymal masses.[50] The imaging characteristics of secondary CNS lymphoma are similar to those seen in PCNSL (Figure 15).

CNS Complications After Chemotherapy and Hematopoietic Stem Cell Transplantation

Neurological complications have serious effects on morbidity and mortality in children undergoing cancer treatment. Acute methotrexate toxicity and complications related to L-asparaginase were discussed above.

Hematopoietic stem cell transplantation (HSCT) is a treatment method that is increasingly employed in the treatment of various malignant and hemotologic diseases in children. Prior to HSCT, high-dose chemotherapy is given to the patient, increasing the likelihood of infectios, vascular, and hemorrhagic complications.

Posterior Reversible Encephalopathy Syndrome

While posterior reversible encephalopathy syndrome (PRES) can be observed in patients with hypertension or eclampsia, patients who are on immunosuppressive medications following organ transplantation are at risk for developing this condition. Although initially described involving the posterior parts of the brain, it can involve the anterior parts of the brain, basal ganglia, brain stem, and cerebellum. Symmetrical cortical and subcortical hyperintense signals are most commonly observed on T2 and FLAIR-W MR images of the parieto-occipital lobes (Figure 16). These areas are often hypointense on T1W MR images and have reduced attenuation on CT scans.[51] Additionally, while generally reversible, the lesions

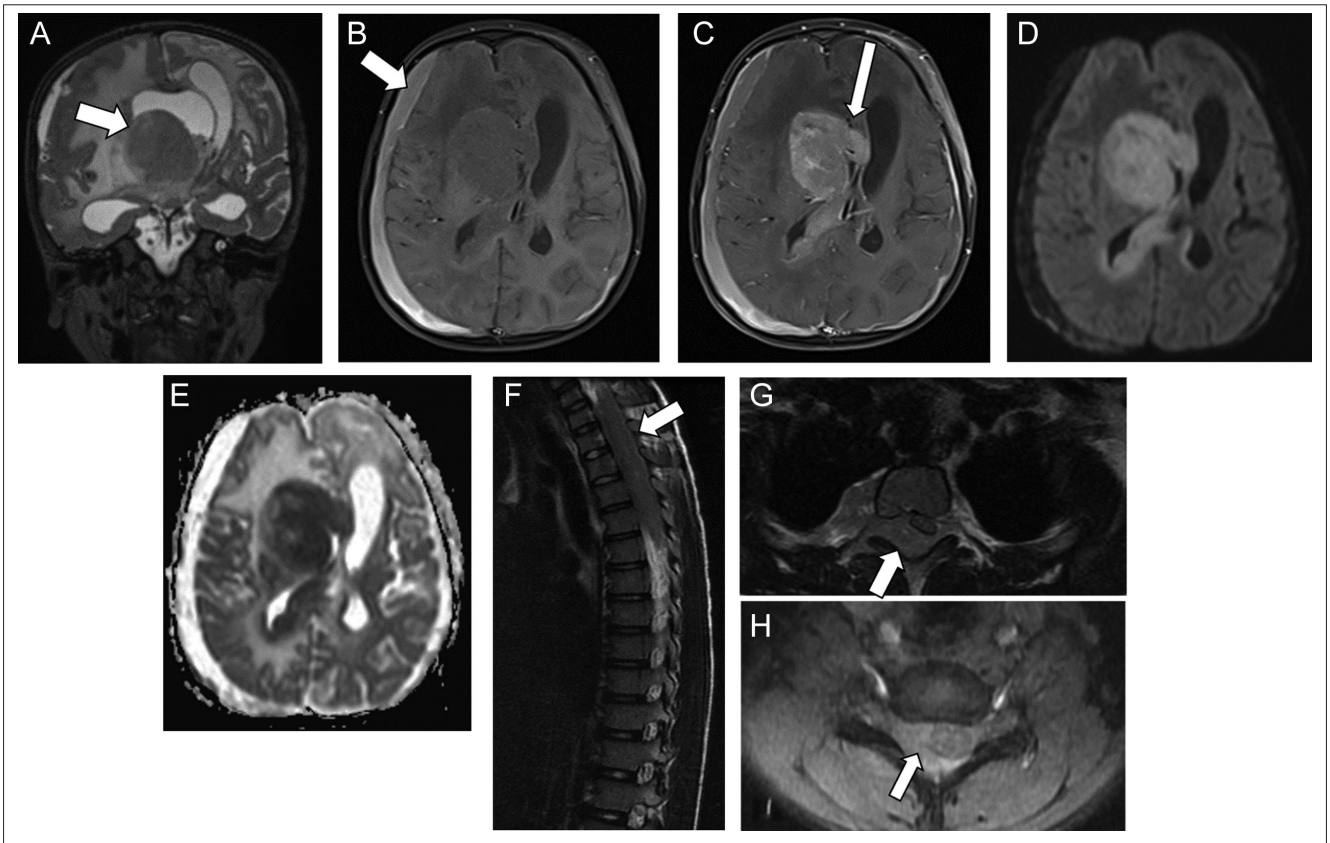

Figure 13. A 4-year-old male diagnosed with primary CNS lymphoma, coronal T2-weighted (T2W) images show a hypointense solid mass involving the basal ganglia and extending into the ventricle in the right frontoparietal white matter (a). Also, right hemispheric subdural effusion and midline shift are seen in pre-contrast T1-weighted (T1W) images (b). There is diffuse heterogeneous enhancement in post-contrast T1W images and the mass extends to the opposite hemisphere through the corpus callosum (c). In diffusion-weighted images (d) and ADC mapping (e), there is diffusion restriction secondary to high cellularity in the mass. 8-year-old male with spinal Burkitt lymphoma, In sagittal T2W images (f), there is a hypointense mass lesion in the spinal canal. In pre- and post-contrast axial images, we see a diffusely enhancing solid mass located extra-axial space in the spinal canal that compresses the spinal cord (g, h).

that show diffusion restriction have a greater likelihood of developing encephalomalacia, gliosis, and volume loss.[52] PRES is believed to be related to a dysfunction of neurovascular autoregulation. Immunosuppressive therapy, hypertension, eclampsia, systemic inflammatory response syndrome, autoimmune diseases, porphyria, and chemotherapy have been reported as causes of PRES.[53] There is usually no correlation between the severity of the clinical findings and lesions observed on MRI.[54]

Cerebrovascular Complications

Vascular complications include arterial occlusion, venous thrombosis, and bleeding. Acute intracranial hemorrhage can result from cancer and cancer therapy. Coagulopathy, platelet count below 10,000/mm^3, and a history of drug use such as prednisolone and treatment with L-asparaginase are among the risk factors.[55] Increased thrombin production due to leukemia, asparaginase and corticosteroids chemotherapy agents, infections, and hereditary prothrombotic diseases are risk

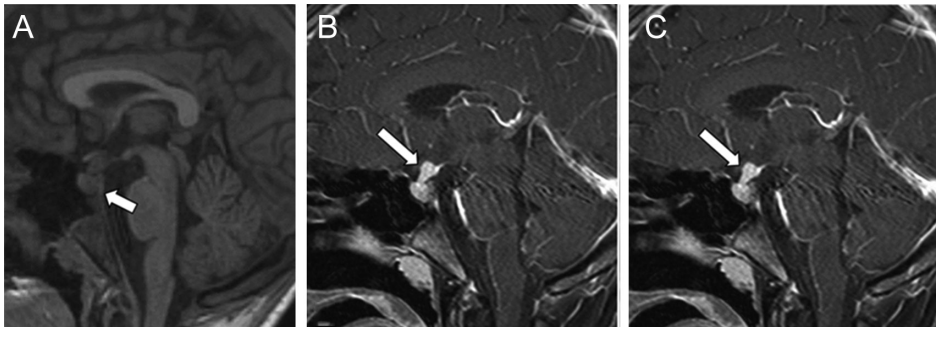

Figure 14. A 15-year-old patient with a diagnosis of diffuse B-cell lymphoma lost the normal hyperintense signal in the neurohypophysis on pre-contrast T1-weighted (T1W) images. Nodular mass thickening was observed in the pituitary stalk on post-contrast T1W images. After the treatment, the thickening of the stalk regressed and the dimensions of the pituitary gland decreased. Normal brightness in the neurohypophysis has not returned.

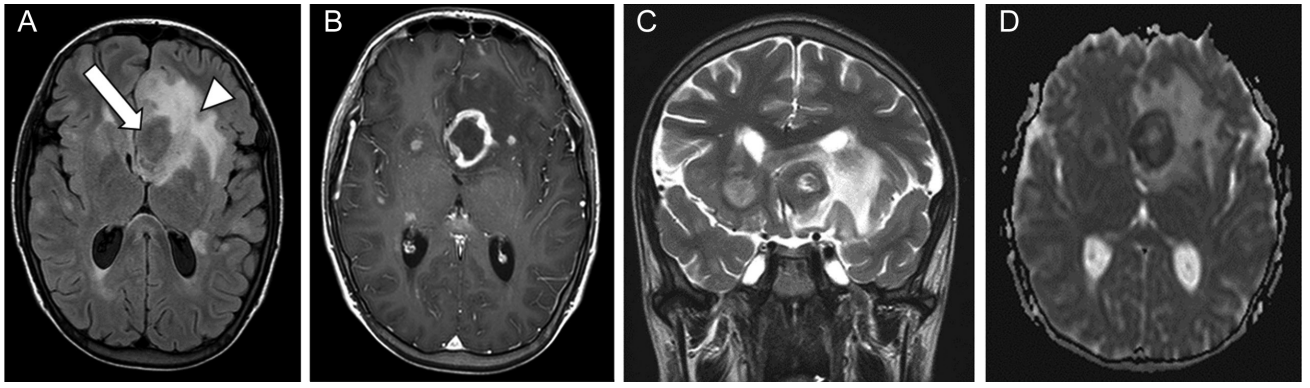

Figure 15. A 15-year-old male with orophayrngeal B-cell lymphoma and central nervous system involvement. In axial FLAIR-W images (a), there is a periventricular mass (arrow) that compresses the 3rd and lateral ventricle, accompanied by a peripheral large edema (arrowhead). Multiple lesions with ring-like enhancements are seen in post-contrast images (b). Midline shift is better seen in coronal T2W images (c) and there is diffusion restriction in ADC mapping (d).

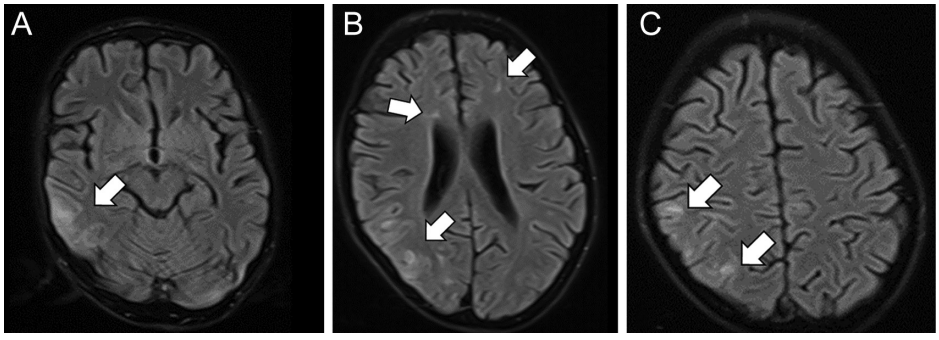

Figure 16. A 16-year-old patient with a diagnosis of thalassemia who underwent bone marrow transplantation, has hyperintense vasogenic edema consistent with PRES in the posterior parietal areas, right temporal lobe, and frontal subcortical areas in FLAIR-W images.

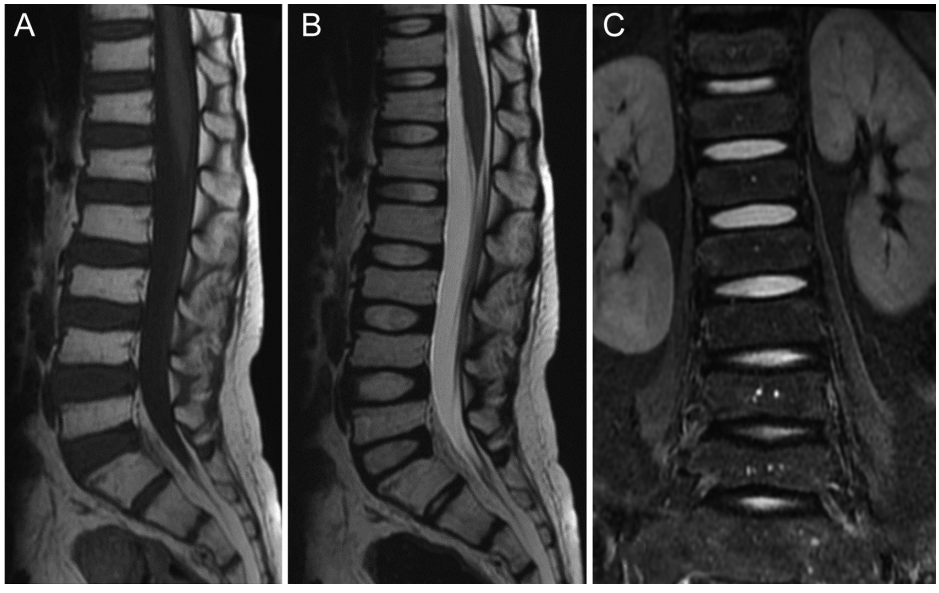

Figure 17. In an 8-year-old patient diagnosed with ALL, hyperintensity in the vertebrae on T1 W (a) and T2W (b), fat-free images and hypointensity secondary to fat suppression on coronal STIR (c) images consistent with fatty bone marrow conversion secondary to radiotherapy are observed. There is also a loss of height secondary to a compression fracture in vetebrae.

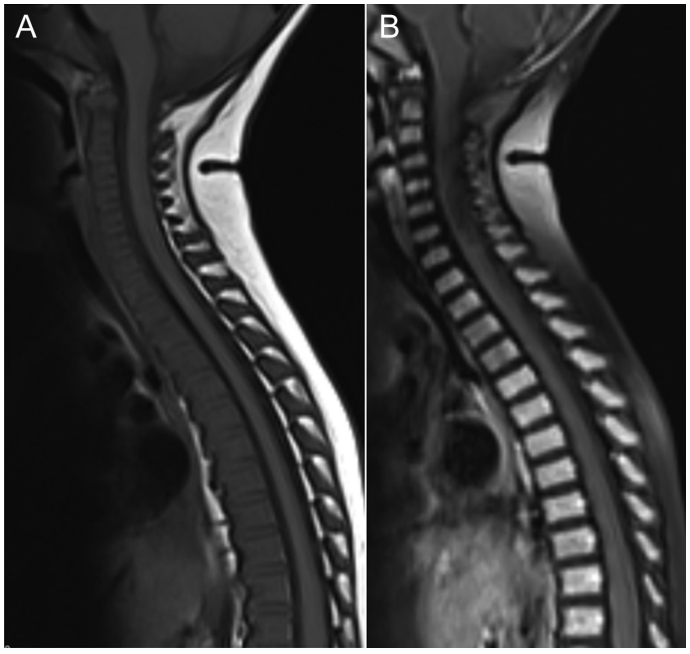

Figure 18. A 1-year-old girl diagnosed with ALL has hypointensity in sagittal T1W (a) and hyperintensity in STIR (b) images, consistent with bone marrow reconstruction.

factors for dural venous sinus thrombosis.[56] Dural venous sinus thrombosis appears as increased density (>70 HU) on noncontrast CT.[57] Contrast-enhanced CT and MR venography (MRV) can be used for evaluation of acute and chronic dural venous sinus thrombosis. However, MRI is preferred as it allows for better evaluation of the parencyma. Addditionally, MRV is preferred in follow-up dural venous thrombosis due to the radiation exposure during CT examinations.[58]

Infectious Complications

Due to immunosuppression after chemotherapy and radiotherapy, the risk of CNS infection increases in the whole body as well. Viral (herpes, cytomegalovirus) and fungal agents are generally responsible for these complications, which are observed as meningoencephalitis or cerebral-cerebellar abscess. Concurrent lung infections are seen in 90% of these patients.[55]

Fungal cerebral abscesses may have central restricted diffusion similar to bacterial abscesses due to highly proteinaceous fluid and cellular infiltration.[59] Because of the systemic distribution of fungal infection, whole body MRI is performed in these patients. MRI should be preferred for imaging, as false negative findings may be present on CT in the early period.

Pediatric cytomegalovirus infection mostly occurs in patients with human immunodeficiency virus infection or after solid organ or bone marrow transplantation. Neurological involvements associated with cytomegalovirus, such as diffuse micronodular encephalitis, ventriculitis, and polyradiculopathy, one of the late complications, were seen in AIDS patients.[60]

Encephalopathies caused by human herpesviruses, especially HHV-6, can be observed 2-6 weeks after bone marrow transplantation. On T2W and FLAIR MR images, bilateral or

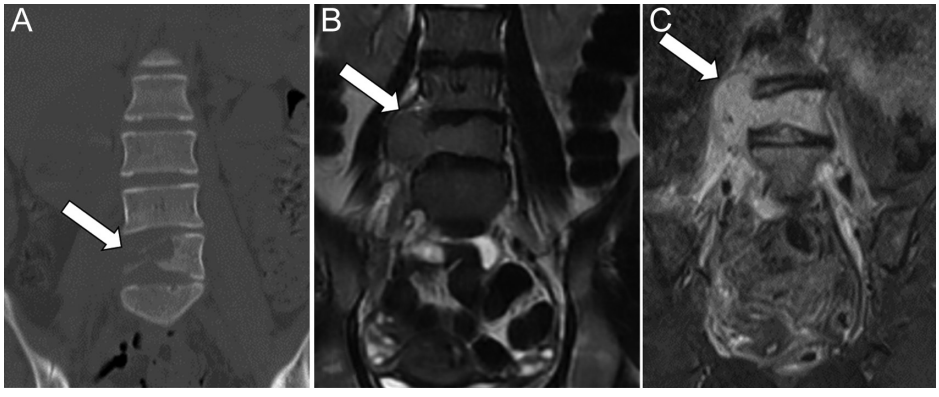

Figure 19. A 15-year-old girl with a diagnosis of primary vertebral diffuse b-cell lymphoma has a solid mass lesion extending to the pre-paravertebral areas, which causes compression by destructing the L4 vertebra on coronal CT (a), T2W (b), and enhanced T1W (c) images.

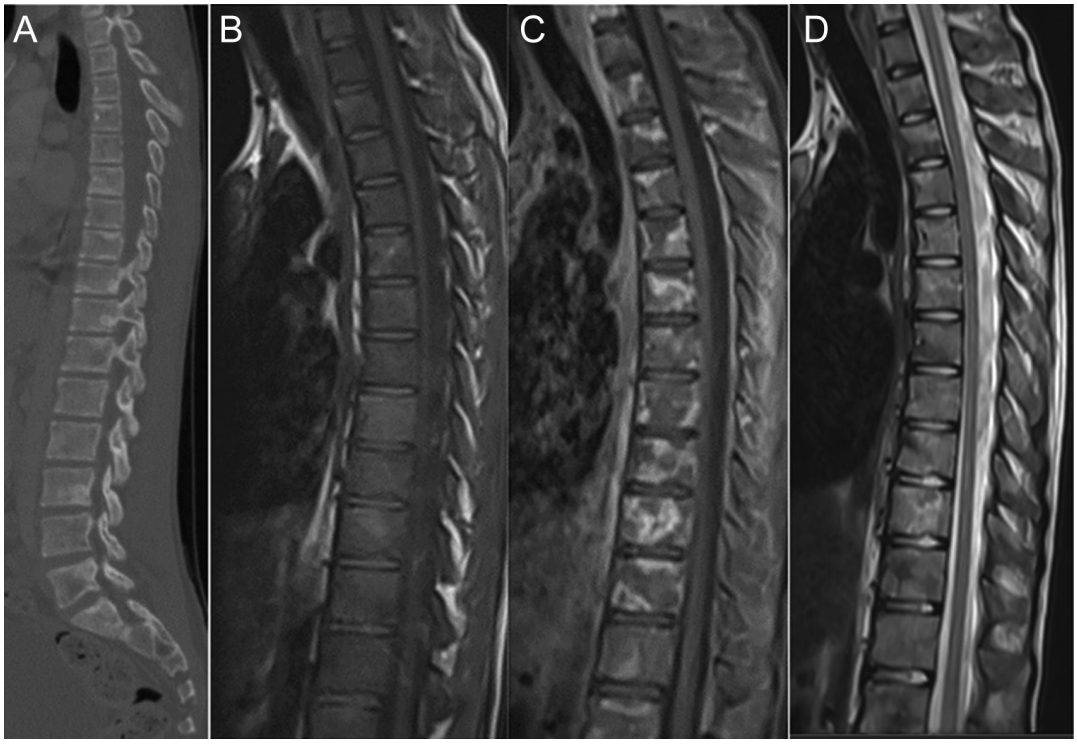

Figure 20. A 17-year-old male was diagnosed with lymphoma. Heterogeneous patchy bone marrow infiltration is observed on sagittal CT (a), pre- (b), and post-contrast (c) T1W and T2W (d) images, respectively.

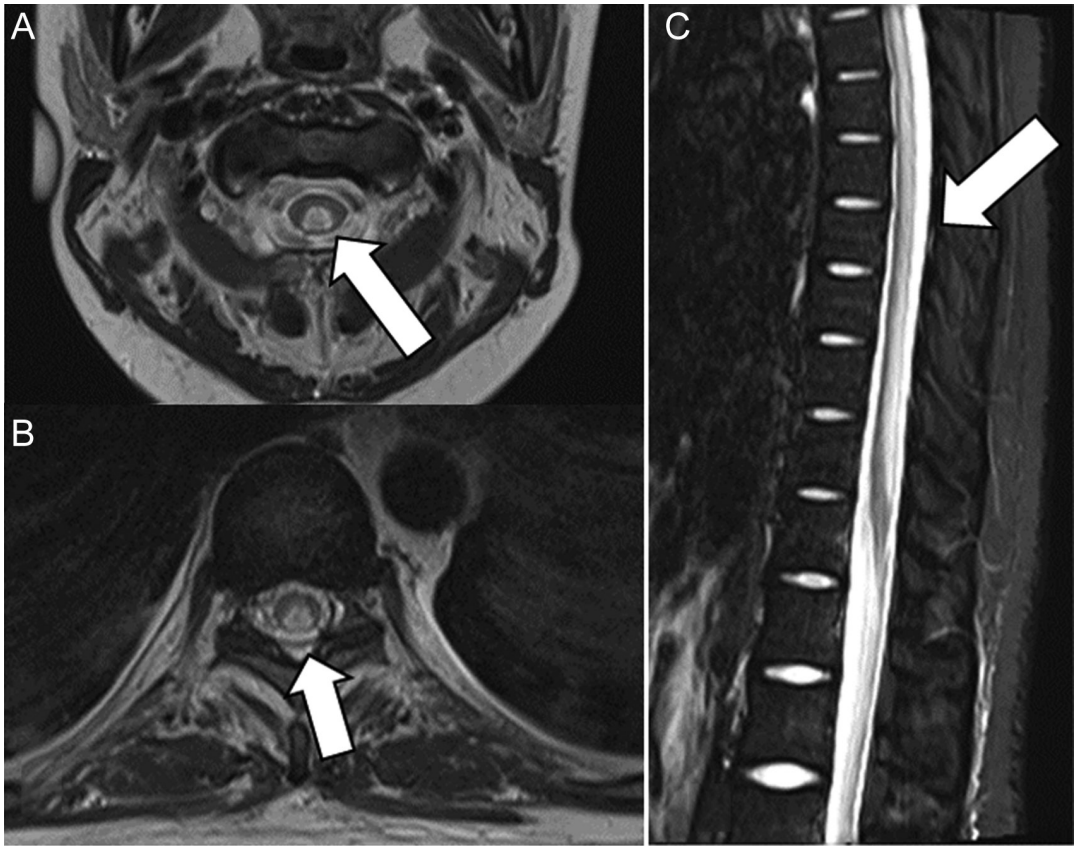

Figure 21. A 14-year-old with T cell lymphoma. Nelarabine neurotoxicity is characterized by nonenhancing, symmetrical T2 prolongation involving the central and posterior spinal cord throughout axial cervical (a), thoracic (b), and sagittal images.

unilateral increased signal intensity is found in the hippocampi, amygdalae, or parahippocampal gyri, usually without diffusion restriction.[61]

NEUROIMAGING OF SPINAL ABNORMALITIES OF HEMATOLOGICAL DISORDERS

Non-neoplastic Disorders

Bone marrow hyperplasia or reconversion occurs in some situations, such as anemia, heart diseases, secondary to treatment. In reconversion, the fatty marrow transforms to red marrow and the T1W signal is reduced. In some cases, paravertebral symmetrical nodular masses may occur as a result of extramedullary hematopoiesis.[62]

In sickle cell anemia and thalassemias, "H-shaped" deformities secondary to collapse in endplates are observed as a result of microvascular infarction. In chronic anemias, secondary to transfusion hematochromatosis may develop, resulting marked T2 hypointensity of the bone marrow related to iron accumulation.[62]

After radiation therapy, the red marrow undergoes fat change and the T1W signal increases. A similar appearance occurs in other bone marrow depletion disorders such as aplastic anemia, but there is involvement throughout the bone marrow as opposed to the focal signal changes seen after radiation therapy where exposure occurs[63] (Figure 17).

Neoplastic Disorders

Fatty bone marrow appears hyperintense on T1W images. Infiltrative processes generally present as diffuse hypointensity on T1W images. In younger children, due to the predominance of hematopoietic marrow, it may be difficult to appreciate the abnormalities on the T1W images, as the expected signal is inherently low. Utilization of Short tau inversion recovery (STIR) images recommended in both young and older children as the cellular infiltrates will generate increased signal and fat within the bone marrow (as expected in older children) will be supressed.[62]

Noncontrast T1W, STIR, and post-contrast fat-suppressed T1W sequences are routinely used in the evaluation of the bone marrow and paraspinal lesions in children.

Leukemia infiltrates the bone marrow diffusely rather than replacing it focally. Focal masses called granulocytic sarcomas may be encountered mostly in myeloid leukemias (Figure 18). MRI of the spine may be normal in approximately 10% of cases with leukemia.

Meningeal/spinal cord involvement is less common. Nodular or diffuse meningeal infiltration can be detected in contrast-enhanced images on MRI. Cerebrospinal fluid sampling is more specific as a normal MRI does not exclude neoplastic meningitis.[64]

Primary vertebral lymphoma is rare. It is mostly observed as metastatic lesions. Non-Hodgkin Lymphoma (NHL) is 3 times more common than others. In Hodgkin's disease, extranodal and vertebral involvement can usually be seen in the late stage (Figure 19). Vertebral involvement in lymphoma is usually in the form of focal lesions. Computed tomography and radiography show increased permeability of the vertebrae or a "moth-eaten" pattern. Focal lesions may be lytic, sclerotic, or mixed. Lesions are slightly hypointense in T1WI and hyperintense in T2WI and may be enhanced. Epidural spread and meningeal involvement can be seen[64] (Figure 20).

Lymphoma is a great imitator and in patients whose primary diagnosis is unclear, it is difficult to distinguish spinal lesions from tuberculosis, sarcoidosis, and other malignancies.[65]

Nelarabine is used in the treatment of T-cell leukemia and lymphoma. Its use is rarely associated with paraplegia and/or sensory problems due to diffuse involvement spinal cord, particularly of the posterior columns[66] (Figure 21).

CONCLUSION

Neuroimaging plays an important role in the diagnosis, but more importantly follow-up of pediatric patients with hematologic diseases and malignancies. Familiarity with the indications of the imaging tests and common imaging manifestations are important in the management of these patients.

Conflict of interest: All authors declare that there is no financial relationship or conflict of interest.

Peer-review: Externally peer-reviewed.

Author Contributions: Concept – S.K., K.K.; Design – S.K.; Supervision – K.K.; Resources – S.K., K.K.; Materials – S.K., K.K.; Data Collection and/or Processing – S.K.; Analysis and/or Interpretation – K.K.; Literature Search – S.K., K.K.; Writing Manuscript – S.K.; Critical Review – K.K.

Declaration of Interests: The authors have no conflict of interest to declare.

Funding: The authors declared that this study has received no financial support.

REFERENCES

1. Filatova I, Stratchko LL, Kanekar S. Central nervous system complications of hemorrhagic and coagulation disorders. *Hematol Oncol Clin North Am.* 2016;30(4):757-777. [CrossRef]
2. McDonald J, Stevenson DA. Hereditary hemorrhagic telangiectasia. *GeneReviews®* [internet]; 2021. https://www.ncbi.nlm.nih.gov/books/NBK1351/. Accessed 2022 Apr 8.
3. Jaskolka J, Wu L, Chan RP, Faughnan ME. Imaging of hereditary hemorrhagic telangiectasia. *AJR Am J Roentgenol.* 2004;183(2):307-314. [CrossRef]
4. Mathew T, Sinha S, Taly AB, Arunodaya GR, Srikanth SG. Neurological manifestations of Ehlers-Danlos syndrome. *Neurol India.* 2005;53(3):339-341. [CrossRef]
5. North KN, Whiteman DAH, Pepin MG, Byers PH. Cerebrovascular complications in Ehlers-Danlos syndrome type IV. *Ann Neurol.* 1995;38(6):960-964. [CrossRef]
6. Sussman JD, Davies-Jones GAB, Neurologic Manifestations of Hematologic Disorders, Aminoff's Neurology and General Medicine. 5th ed. Academic Press; 2014: Chapter 25 505-537. ISBN 9780124077102, (https://www.sciencedirect.com/science/article/pii/B9780124077102000254) [CrossRef]
7. Clouse LH, Comp PC. The regulation of hemostasis: the protein C system. *N Engl J Med.* 1986;314(20):1298-1304. [CrossRef]

8. Dahlbäck B, Villoutreix BO. The anticoagulant protein C pathway. *FEBS Lett*. 2005;579(15):3310-3316. [CrossRef]
9. Bick RL, Pegram M. Syndromes of hypercoagulability and thrombosis: a review. *Semin Thromb Hemost*. 1994;20(1):109-132. [CrossRef]
10. Hayashida M, Yamada H, Yamazaki S, et al. Combined protein C and protein S deficiency in a family with repetitive thromboembolism and segregated gene mutations. *Intern Med*. 2003;42(3):268-272. [CrossRef]
11. Piel FB, Steinberg MH, Rees DC. Sickle cell disease. Longo DL, editor. *N Engl J Med*. 2017;376(16):1561-1573. [CrossRef]
12. Powars D, Weidman JA, Odom-Maryon T, et al. Sickle cell chronic lung disease: prior morbidity and the risk of pulmonary failure. *Medicine (United States)*. 1988;67(1):66-76.
13. Moran CJ, Siegel MJ, Debaun MR. Sickle cell disease: imaging of cerebrovascular complications. *Radiology*. 1998;206(2):311-321. [CrossRef]
14. Adams RJ, McKie VC, Carl EM, et al. Long-term stroke risk in children with sickle cell disease screened with transcranial Doppler. *Ann Neurol*. 1997;42(5):699-704. [CrossRef]
15. Saito N, Nadgir RN, Flower EN, Sakai O. Clinical and radiologic manifestations of sickle cell disease in the head and neck. *RadioGraphics*. 2010;30(4):1021-1034. [CrossRef]
16. Scott RM, Smith ER. Moyamoya disease and Moyamoya syndrome. *N Engl J Med*. 2009;360(12):1226-1237. [CrossRef]
17. Smith ER, Scott RM. Progression of disease in unilateral Moyamoya syndrome. *Neurosurg Focus*. 2008;24(2):E17. [CrossRef]
18. Thangarajh M, Yang G, Fuchs D, et al. Magnetic resonance angiography-defined intracranial vasculopathy is associated with silent cerebral infarcts and glucose-6-phosphate dehydrogenase mutation in children with sickle cell anaemia. *Br J Haematol*. 2012;159(3):352-359. [CrossRef]
19. Dowling MM, Quinn CT, Plumb P, et al. Acute silent cerebral ischemia and infarction during acute anemia in children with and without sickle cell disease. *Blood*. 2012;120(19):3891-3897. [CrossRef]
20. Hajimoradi M, Haseli S, Abadi A, Chalian M. Musculoskeletal imaging manifestations of beta-thalassemia. *Skelet Radiol*. 2021;50(9):1749-1762. [CrossRef]
21. Toumba M, Skordis N. Osteoporosis syndrome in thalassaemia major: an overview. *J Osteoporos*. 2010;2010:537673. [CrossRef]
22. Karimi M, Haghpanah S, Bagheri MH, Bordbar MR, Pishdad P, Rachmilewitz EA. Frequency and distribution of asymptomatic brain lesions in patients with β-thalassemia intermedia. *Ann Hematol*. 2012;91(12):1833-1838. [CrossRef]
23. Taher AT, Musallam KM, Nasreddine W, Hourani R, Inati A, Beydoun A. Asymptomatic brain magnetic resonance imaging abnormalities in splenectomized adults with thalassemia intermedia. *J Thromb Haemost*. 2010;8(1):54-59. [CrossRef]
24. Qiu D, Chan GCF, Chu J, et al. MR quantitative susceptibility imaging for the evaluation of iron loading in the brains of patients with β-thalassemia major. *AJNR Am J Neuroradiol*. 2014;35(6):1085-1090. [CrossRef]
25. Akhlaghpoor S, Ghahari A, Morteza A, Khalilzadeh O, Shakourirad A, Alinaghizadeh MR. Quantitative T2* magnetic resonance imaging for evaluation of iron deposition in the brain of β-thalassemia patients. *Clin Neuroradiol*. 2012;22(3):211-217. [CrossRef]
26. Metafratzi Z, Argyropoulou MI, Kiortsis DN, Tsampoulas C, Chaliassos N, Efremidis SC. T(2) relaxation rate of basal ganglia and cortex in patients with beta-thalassaemia major. *Br J Radiol*. 2001;74(881):407-410. [CrossRef]
27. Arceci RJ, Hann IM, Smith OP. Pediatric Hematology. *John Wiley and Sons*. 3rd ed; 2007:1-826. [CrossRef]
28. Prayer D, Grois N, Prosch H, Gadner H, Barkovich AJ. MR imaging presentation of intracranial disease associated with Langerhans cell histiocytosis. *AJNR Am J Neuroradiol*. 2004;25(5):880-891.
29. Turcu AF, Erickson BJ, Lin E, et al. Pituitary stalk lesions: the Mayo Clinic experience. *J Clin Endocrinol Metab*. 2013;98(5):1812-1818. [CrossRef]
30. Kershenovich A, Price AV v., Koral K, Goldman S, Swift DM. Failure to treat obstructive hydrocephalus with endoscopic third ventriculostomy in a patient with neurodegenerative Langerhans cell histiocytosis. *J Neurosurg Pediatr*. 2008;2(5):304-309. [CrossRef]
31. Malik P, Antonini L, Mannam P, et al. MRI patterns in pediatric CNS hemophagocytic lymphohistiocytosis. *AJNR Am J Neuroradiol*. 2021;42(11):2077-2085. [CrossRef]
32. Voskoboinik I, Smyth MJ, Trapani JA. Perforin-mediated target-cell death and immune homeostasis. *Nat Rev Immunol*. 2006;6(12):940-952. [CrossRef]
33. Rabin KR, Margolin JF, Kamdar KY, Poplack DG. Leukemias and lymphomas of childhood. In: DeVita VT, Lawrence TS, Rosenberg SA, eds. *DeVita, Hellman, and Rosenberg's Cancer: Principles and Practice of Oncology*. 10th ed. Philadelphia, PA: Lippincott Williams & Wilkins; 2015.
34. Parker BR. Leukemia and lymphoma in childhood. *Radiol Clin North Am*. 1997;35(6):1495-1516.
35. Laningham FH, Kun LE, Reddick WE, Ogg RJ, Morris EB, Pui CH. Childhood central nervous system leukemia: historical perspectives, current therapy, and acute neurological sequelae. *Neuroradiology*. 2007;49(11):873-888. [CrossRef]
36. Singh A, Kumar P, Chandrashekhara SH, Kumar A. Unravelling chloroma: review of imaging findings. *Br J Radiol*. 2017;90(1075):20160710. [CrossRef]
37. Kembhavi SA, Somvanshi S, Banavali S, Kurkure P, Arora B. Pictorial essay: acute neurological complications in children with acute lymphoblastic leukemia. *Indian J Radiol Imaging*. 2012;22(2):98-105. [CrossRef]
38. Ulu EM, Töre HG, Bayrak A, Güngör D, Coşkun M. *MRI of central nervous system abnormalities in childhood leukemia*; 2009 Jun;15(2):86-92. PMID: 19517377.
39. Rollins N, Winick N, Bash R, Booth T. Acute methotrexate neurotoxicity: findings on diffusion-weighted imaging and correlation with clinical outcome. *AJNR Am J Neuroradiol*. 2004;25(10):1688-1695.
40. Malhotra P, Jain S, Kapoor G. Symptomatic cerebral Sinovenous thrombosis associated with L-asparaginase in children with acute lymphoblastic leukemia: a single institution experience over 17 years. *J Pediatr Hematol Oncol*. 2018;40(7):e450-e453. [CrossRef]
41. Porto L, Kieslich M, Schwabe D, Zanella FE, Lanfermann H. Central nervous system imaging in childhood leukaemia. *Eur J Cancer*. 2004;40(14):2082-2090. [CrossRef]
42. Finelli PF, Foxman EB. The etiology of ring lesions on diffusion-weighted imaging. *Neuroradiol J*. 2014;27(3):280-287. [CrossRef]
43. Chan BY, Gill KG, Rebsamen SL, Nguyen JC. MR imaging of pediatric bone marrow. *RadioGraphics*. 2016;36(6):1911-1930. [CrossRef]
44. Chen CY, Zimmerman RA, Faro S, Bilaniuk LT, Chou TY, Molloy PT. Childhood leukemia: central nervous system abnormalities during and after treatment. *AJNR Am J Neuroradiol*. 1996;17(2):295-310.
45. Haldorsen IS, Kråkenes J, Krossnes BK, Mella O, Espeland A. CT and MR imaging features of primary central nervous system lymphoma in Norway, 1989-2003. 2009. Available at: [CrossRef]. Accessed 2022 Apr 9.
46. Abla O, Weitzman S. Primary central nervous system lymphoma in children. *Neurosurg Focus*. 2006;21(5):E8-E8. [CrossRef]
47. Zhang S, Li H, Zhu R, Zhang M. Application value of magnetic resonance imaging in diagnosing central nervous system lymphoma. *Pak J Med Sci*. 2016;32(2):389-393. [CrossRef]
48. Camacho DLA, Smith JK, Castillo M. Differentiation of toxoplasmosis and lymphoma in AIDS patients by using apparent diffusion coefficients. *AJNR Am J Neuroradiol*. 2003;24(4):633-637.
49. Pui CH, Thiel E. Central nervous system disease in hematologic malignancies: historical perspective and practical applications. *Semin Oncol*. 2009;36(4):S2-S16. [CrossRef]

50. Gleissner B, Chamberlain M. Treatment of CNS dissemination in systemic lymphoma. *J Neurooncol.* 2007;84(1):107-117. [CrossRef]
51. McKinney AM, Jagadeesan BD, Truwit CL. Central-variant posterior reversible encephalopathy syndrome: brainstem or basal ganglia involvement lacking cortical or subcortical cerebral edema. *AJR Am J Roentgenol.* 2013;201(3):631-638. [CrossRef]
52. Covarrubias DJ, Luetmer PH, Campeau NG. Posterior reversible encephalopathy syndrome: prognostic utility of quantitative diffusion-weighted MR images. *AJNR Am J Neuroradiol.* 2002;23(6):1038-1048.
53. Bartynski WS. Posterior reversible encephalopathy syndrome, Part 2: controversies surrounding pathophysiology of vasogenic edema. *AJNR Am J Neuroradiol.* 2008;29(6):1043-1049. [CrossRef]
54. Fugate JE, Claassen DO, Cloft HJ, Kallmes DF, Kozak OS, Rabinstein AA. Posterior reversible encephalopathy syndrome: associated clinical and radiologic findings. *Mayo Clin Proc.* 2010;85(5):427-432. [CrossRef]
55. Kaste SC, Rodriguez-Galindo C, Furman WL, Langston J, Thompson SJ. Imaging aspects of neurologic emergencies in children treated for non-CNS malignancies. *Pediatr Radiol.* 2000;30(8):558-565. [CrossRef]
56. Kieslich M, Porto L, Lanfermann H, Jacobi G, Schwabe D, Böhles H. Cerebrovascular complications of L-asparaginase in the therapy of acute lymphoblastic leukemia. *J Pediatr Hematol Oncol.* 2003;25(6):484-487. [CrossRef]
57. Black DF, Rad AE, Gray LA, Campeau NG, Kallmes DF. Cerebral venous sinus density on noncontrast CT correlates with hematocrit. *AJNR Am J Neuroradiol.* 2011;32(7):1354-1357. [CrossRef]
58. Vázquez E, Lucaya J, Castellote A, et al. Neuroimaging in pediatric leukemia and lymphoma: differential diagnosis. *RadioGraphics.* 2002;22(6):1411-1428. [CrossRef]
59. Gaviani P, Schwartz RB, Hedley-Whyte ET, et al. Diffusion-weighted imaging of fungal cerebral infection. *AJNR Am J Neuroradiol.* 2005;26(5):1115-1121.
60. Arribas JR, Storch GA, Clifford DB, Tselis AC. Cytomegalovirus encephalitis. *Ann Intern Med.* 1996;125(7):577-587. [CrossRef]
61. Baskin HJ, Hedlund G. Neuroimaging of herpesvirus infections in children. *Pediatr Radiol.* 2007;37(10):949-963. [CrossRef]
62. Pawha PS, Chokshi FH. Imaging of spinal manifestations of hematological disorders. *Hematol Oncol Clin North Am.* 2016;30(4):921-944. [CrossRef]
63. Cavenagh EC, Weinberger E, Shaw DWW, White KS, Geyer JR. Hematopoietic marrow regeneration in pediatric patients undergoing spinal irradiation: MR depiction. *AJNR Am J Neuroradiol.* 1995;16(3):461-467.
64. Alyas F, Saifuddin A, Connell D. MR imaging evaluation of the bone marrow and marrow infiltrative disorders of the lumbar spine. *Magn Reson Imaging Clin N Am.* 2007;15(2):199-219, vi. [CrossRef]
65. Do-Dai DD, Brooks MK, Goldkamp A, Erbay S, Bhadelia RA. Magnetic resonance imaging of intramedullary spinal cord lesions: a pictorial review. *Curr Probl Diagn Radiol.* 2010;39(4):160-185. [CrossRef]
66. Madhavan AA, Carr CM, Alkhateeb H, Staff NP, Naddaf E. Nelarabine-induced myelotoxicity. *Neurology.* 2021;96(4):175-176. [CrossRef]